Analogues of the Iron-binding Site in Catechol 1,2-Dioxygenase: Iron(III) Complexes of Benzimidazole- and Pyridine-containing Tridentate Ligands†

Rathinam Viswanathan and Mallayan Palaniandavar*
Department of Chemistry, Bharathidasan University, Tiruchirappalli 620 024, Tamil Nadu, India

A series of iron(III) complexes of the type $[FeLCl_2]\cdot H_2O$ [HL = *N*-(pyridin-2-ylmethyl)salicylideneamine, (2-hydroxy-5-nitrobenzyl)(pyridin-2-ylmethyl)amine, (2-hydroxy-5-nitrobenzyl)(2-pyridin-2-ylethyl)-amine, *N*-(2-imidazol-4-ylethyl)salicylideneamine, *N*-(benzimidazole-2-ylmethyl)salicylaldimine, (benzimidazol-2-ylmethyl)(2-hydroxybenzyl)amine, or (benzimidazol-2-ylmethyl)(2-hydroxy-5-nitrobenzyl)amine] have been prepared. Also $[FeLCl_3]\cdot H_2O$ [L = bis(benzimidazol-2-ylmethyl)amine] has been isolated. These complexes have been characterised using IR, UV/VIS and EPR spectral and electrochemical techniques. Their interaction with a variety of mono- and bi-dentate heterocyclic bases as well as phenols has been investigated using electronic and EPR spectroscopy. Their interaction with 3,5-di-*tert*-butylcatechol (H_2dbcat) and its anions reveals changes in the phenolate-to-iron(III) charge-transfer (c.t.) band similar to those for catechol dioxygenase–substrate complexes. The redox behaviour of the iron(III) complexes and their 1 : 1 adducts with dbcat anions generated *in situ* has been investigated in methanol. There is a linear correlation between the Fe^{III}–Fe^{II} redox potential and the c.t. band energy of the complexes. All the complexes catalyse the oxidative cleavage of H_2dbcat by molecular oxygen to yield *cis,cis*-muconic anhydride. The catalytic activity has been correlated with the Fe^{III}–Fe^{II} as well as $dbsq^{\cdot}$–H_2dbcat (dbsq = 3,5-di-*tert*-butyl-1,2-benzosemiquinone) redox potentials of the dbcat adducts.

Catechol 1,2-dioxygenase (CTD) and protocatechuate 3,4-dioxygenase (PCD) are bacterial non-haem iron enzymes which catalyse the oxidative cleavage of catechols to *cis,cis*-muconic (hexa-2,4-dienedioic) acids *via* a mechanism involving a high-spin iron(III) centre.[1] The EPR spectra of these enzymes reveal a signal at $g = 4.3$, characteristic of a high-spin iron(III) centre in a rhombic environment.[2] Based on various spectroscopic studies, the active sites of these enzymes have been proposed[3–6] to consist of iron(III) co-ordinated to two tyrosines, two histidines, and a water molecule. Recent resonance-Raman studies[7,8] have shown that the co-ordination of tyrosines is not affected by substrate or oxygen binding and that the iron remains in the oxidation state III throughout the course of the catalytic reaction. The co-ordination of tyrosine gives rise to phenolate-to-iron(III) charge transfer which persists throughout the reaction cycle, even in the short-lived intermediates observed with stopped-flow kinetic methods.[9]

Several co-ordination complexes have been designed[10–14] to model the iron active sites in iron dioxygenases; however, models which mimic both the catalytic activity and spectral behaviour are scarce.[14] Que has extensively studied several iron(III) complexes[15] as models and proposed a substrate rather than oxygen-activation mechanism[16] for the catalysis. In this novel scheme, the substrate catechol loses both its protons upon co-ordination to the iron site and becomes susceptible to reaction with oxygen to yield a peroxide intermediate which then decomposes to product. The product yields and reactivity have been shown to depend on the Lewis acidity of the iron centre in a series of iron(III) complexes[16] of tripodal ligands with CO_2^- functionalities. Only two[14,16] of the functional models reported so far contain the co-ordinated phenolate donor and another model[17] both the established imidazole-derived nitrogen and phenolate donors in CTD. So we became interested in constructing and studying functional models for CTD, incorporating tridentate ligands containing both these functionalities. Such a study would provide further information pertinent to an improved understanding of structure *vs.* spectra correlations, and the function and reactivity of the active site. In the present report models involving tridentate ligands (HL^1–HL^7 and L^8) are discussed. In principle, they make available *cis*-co-ordination positions for adduct formation and so are very convenient for investigating the effect of substrate binding on spectra. Spectroscopic, electrochemical and reactivity data are presented for a series of systematically modified model compounds.

Experimental

Materials.—Iron(III) chloride (anhydrous) and triethylamine (SD Fine Chemicals, India) were analytical grade reagents used as supplied. *o*-Phenylenediamine, β-alanine, salicylaldehyde (BDH), 2,2′-bipyridine (Merck), sodium tetrahydroborate, *N*-methylimidazole (Fluka), 1,10-phenanthroline (LOBA), catechol, 3,5-di-*tert*-butylcatechol (H_2dbcat) (Aldrich) and 2,9-dimethyl-1,10-phenanthroline (GFS) were used as received. 2-Chloromethylbenzimidazole (Fluka) and 2-chloromethylpyridine hydrochloride (Aldrich) were used as received. The supporting electrolyte tetrahexylammonium perchlorate (GFS) was recrystallised twice from aqueous ethanol.

Syntheses of Ligands.—2-Aminomethylbenzimidazole dihydrochloride,[18] 2-hydroxy-5-nitrobenzyl chloride[19] and bis(benzimidazol-2-ylmethyl)amine[20] (HL^9) were synthesised by published procedures.

Syntheses of Iron(III) Complexes.—The complexes $[FeL^4Cl_2]\cdot H_2O$[21] {HL^4 = *N*-[2-(imidazol-4-ylethyl)]salicylideneamine} and $[FeL^8Cl_3]$[22] were prepared as reported earlier.

$[FeL^1Cl_2]\cdot H_2O$ [HL^1 = N-(*pyridin-2-ylmethyl*)*salicylideneamine*]. To a solution of 2-aminomethylpyridine (0.44 g, 4

† *Non-SI units employed:* $\mu_B \approx 9.27 \times 10^{-24}$ JT^{-1}, eV $\approx 1.60 \times 10^{-19}$ J, G = 10^{-4} T.

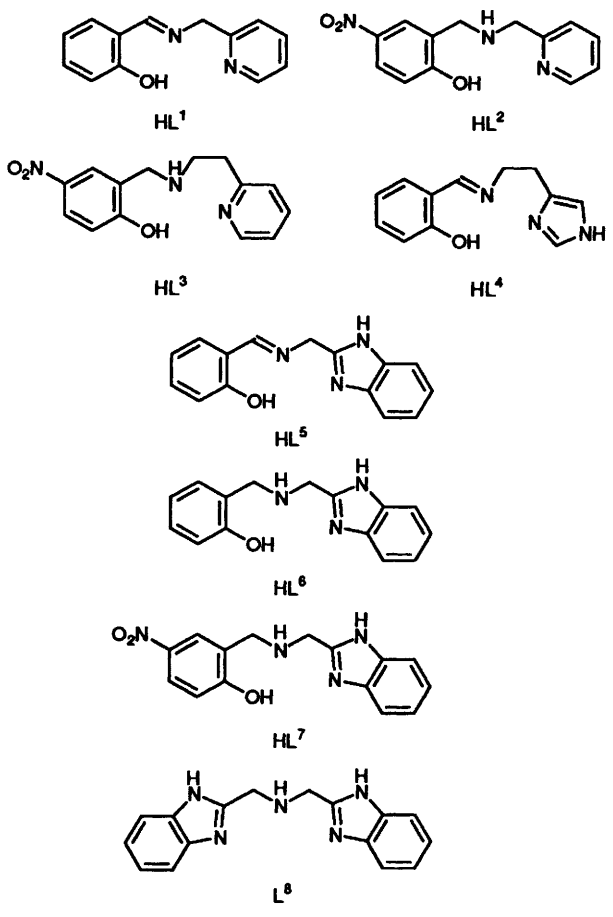

mmol) in tetrahydrofuran (thf) (25 cm^3) was added salicylaldehyde (0.49 g, 4 mmol) and refluxed for 30 min. The mixture was then cooled and filtered. To the filtrate NEt_3 (0.405 g, 4 mmol) and then $FeCl_3$ (0.65 g, 4 mmol) in methanol (5 cm^3) were added and the solution cooled. The precipitate obtained was filtered off, washed with small amounts of cold methanol and dried under vacuum. Yield 0.28 g (78%) (Found: C, 43.65; H, 3.40; N, 7.60. Calc. for $C_{13}H_{13}Cl_2FeN_2O_2$: C, 43.85; H, 3.70; N, 7.85%).

$[FeL^2Cl_2]\cdot H_2O$ [HL^2 = (*2-hydroxy-5-nitrobenzyl*)(*pyridin-2-ylmethyl*)*amine*]. To a solution of 2-hydroxy-5-nitrobenzyl chloride (0.75 g, 4 mmol) in thf (50 cm^3) were added 2-aminomethylpyridine (0.44 g, 4 mmol) and then NEt_3 (0.81 g, 8 mmol) and refluxed for 2 h. The mixture was then cooled and filtered. To the filtrate, $FeCl_3$ (0.65 g, 4 mmol) in methanol was added. The brown precipitate obtained was filtered off, washed with small amounts of cold methanol and dried under vacuum. Yield 1.42 g (89%) (Found: C, 38.60; H, 3.35; N, 10.50. Calc. for $C_{13}H_{14}Cl_2FeN_3O_4$: C, 38.75; H, 3.50; N, 10.45%).

$[FeL^3Cl_2]\cdot H_2O$ [HL^3 = (*2-hydroxy-5-nitrobenzyl*)(*2-pyridin-2-ylethyl*)*amine*]. To a solution of 2-hydroxy-5-nitrobenzyl chloride (0.75 g, 4 mmol) in methanol (50 cm^3) was added 2-aminoethylpyridine (0.44 g, 4 mmol) in methanol (25 cm^3) and refluxed for 30 min. The solution was cooled, filtered and then NEt_3 (0.41 g, 4 mmol) was added followed by $FeCl_3$ (0.65 g, 4 mmol). The precipitate obtained on cooling was filtered off, washed with small amounts of cold methanol and dried under vacuum. Yield 1.20 g (72%) (Found: C, 40.30; H, 3.85; N, 10.05. Calc. for $C_{14}H_{16}Cl_2FeN_3O_4$: C, 40.30; H, 3.85; N, 10.10%).

$[FeL^5Cl_2]\cdot H_2O$ [HL^5 = N-(*benzimidazole-2-ylmethyl*)-*salicylideneamine*]. To a solution of 2-aminomethylbenzimidazole dihydrochloride (0.88 g, 4 mmol) in methanol (25 cm^3) was added salicylaldehyde (0.49 g, 4 mmol) with stirring. To this solution NEt_3 (1.22 g, 12 mmol) was added and refluxed for 30 min. The mixture was then cooled and filtered. To the filtrate $FeCl_3$ (0.65 g, 4 mmol) in methanol (5 cm^3) was added and stirred. The violet precipitate obtained was filtered off, washed with small amounts of cold methanol and dried under vacuum. Yield 1.25 g (79.6%) (Found: C, 45.80; H, 3.80; N, 10.50. Calc. for $C_{15}H_{14}Cl_2FeN_3O_2$: C, 45.60; H, 3.55; N, 10.65%).

$[FeL^6Cl_2]\cdot H_2O$ [HL^6 = (*benzimidazol-2-ylmethyl*)(*2-hydroxybenzyl*)*amine*]. To a solution of 2-aminomethylbenzimidazole dihydrochloride (0.88 g, 4 mmol) in methanol (25 cm^3) was added with stirring sodium hydroxide (0.16 g, 4 mmol) in methanol (4 cm^3). After adding salicylaldehyde (0.49 g, 4 mmol) the solution was refluxed for 30 min. To the cooled solution $NaBH_4$ (0.15 g, 4 mmol) was added with stirring until the solution became colourless and then the solvent was rotaevaporated. To the filtrate was added $FeCl_3$ (0.65 g, 4 mmol) in methanol (5 cm^3), and the solution was cooled and filtered. A violet precipitate was obtained on adding water to the filtrate. This was filtered off, washed with cold methanol and dried under vacuum. Yield 1.4 g (82%) (Found: C, 45.75; H, 3.80; N, 10.40. Calc. for $C_{15}H_{16}Cl_2FeN_3O_2$: C, 45.35; H, 4.05; N, 10.60%).

$[FeL^7Cl_2]\cdot H_2O$ [HL^7 = (*benzimidazol-2-ylmethyl*)(*2-hydroxy-5-nitrobenzyl*)*amine*]. To a solution of 2-hydroxy-5-nitrobenzyl chloride (0.75 g, 4 mmol) in methanol (50 cm^3) was added 2-aminomethylbenzimidazole dihydrochloride (0.44 g, 2 mmol). To this solution NEt_3 (0.81 g, 8 mmol) was added and refluxed for 2 h. This was then cooled and filtered. To the filtrate $FeCl_3$ (0.33 g, 2 mmol) in methanol (20 cm^3) was added. The solid obtained on adding water to the filtrate was filtered off, washed with cold methanol and dried under vacuum. Yield 0.85 g (77%) (Found: C, 40.80; H, 3.20; N, 12.90. Calc. for $C_{15}H_{15}Cl_2FeN_4O_4$: C, 40.75; H, 3.40; N, 12.65%).

Physical Measurements.—Elemental analyses were performed at Hindustan Photo Film Manufacturing Co., Ootacamund and Regional Sophisticated Instrumentation Centre, Lucknow, India. Conductivity measurements in methanol solution (≈ 1 mmol dm^{-3} complex) were carried out using an Elico PE 133 pH/conductivity meter and a cell of cell constant 1.0. Infrared spectra were recorded on a Shimadzu 435 spectrophotometer using a 2 cm^{-1} standard resolution, electronic spectra on Hitachi U-3410 double-beam UV-VIS-NIR and Perkin-Elmer Lambda 3B spectrophotometers and EPR spectra on a Varian E 112 X-band spectrometer, the field being calibrated with diphenylpicrylhydrazyl (dpph). All voltammetric experiments were performed in a single-compartment cell with a three-electrode system on a EG & G PAR 273 potentiostat/galvanostat equipped with an IBM PS/2 computer and a HIPLOT DMP-40 series digital plotter. The working electrode was a platinum sphere (area 0.378 cm^2) and the reference electrode saturated calomel. A platinum plate was used as the counter electrode. The supporting electrolyte used was 0.1 mol dm^{-3} $N(C_6H_{13})_4ClO_4$. The concentration of the complexes in methanol solutions was ≈ 1 mmol dm^{-3}. Solutions were deoxygenated by purging with N_2 gas for 15 min prior to measurements and during measurements a stream of N_2 was passed over the solution. The temperature of the methanol solution was maintained at 25 ± 0.2 °C by a Haake D8 G circulating bath. The potential of the ferrocene–ferrocenium couple (0.100 V, $Ag–Ag^+$) was measured in methanol under the same conditions to enable correction for junction potentials.

Reactivity Studies.—The following typical procedure[14] was employed to study the dioxygenase activity of model compounds. A mixture of 3,5-di-*tert*-butylcatechol (1 mmol) and the iron(III) complex (0.02 mmol) in nitromethane solution (10 cm^3) was left in contact with air at room temperature for 4 d. The product was isolated by column chromatography on silica gel using chloroform as eluent and was identified as *cis,cis*-muconic anhydride[23] [m.p. 93–95 °C, ν(C=O) 1745 and 1765 cm^{-1}, λ_{max} 247 nm].

Table 1 Electronic spectral data[a] for iron(III) complexes and their adducts in methanol solution

Added ligand[b,c]	λ_{max}/nm (ε/dm^3 mol^{-1} cm^{-1})		
	$[FeL^1Cl_2]\cdot H_2O$	$[FeL^2Cl_2]\cdot H_2O$	$[FeL^5Cl_2]\cdot H_2O$
None	543 (400), 436 (sh) (320), 323 (1670)	478 (450), 392 (840), 355 (1400), 313 (1700)	554 (1630), 425 (sh) (1380), 330 (6280)
mim	492 (380), 405 (sh) (550), 330 (1520)	473 (230), 388 (890), 351 (1390)	460 (1380), 414 (sh) (1710)
bzim	511 (430), 415 (sh) (450), 330 (1660)	478 (80), 397 (280), 352 (390)	496 (1400), 420 (sh) (1710), 310 (8380)
py	462 (270), 415 (sh) (350), 310 (sh) (1280)	470 (300), 390 (sh) (2000), 358 (3480)	505 (1870), 414 (1700), 326 (8260)
Pho^-	467 (130), 376 (sh) (560), 335 (sh) (370), 326 (sh) (510)	390 (390), 334 (6230), 326 (6720), 318 (6410)	382 (3820)
sal^-[d]	483 (120), 374 (2680), 332 (2460)	326 (1760)	673 (sh) (250), 370 (1630)
bipy	510 (860), 487 (sh) (900), 380 (sh) (820), 330 (sh) (1840)	480 (530), 391 (sh) (1770), 350 (2490)	515 (6890), 490 (6290), 373 (4250), 325 (8690)
phen	507 (470), 487 (sh) (430), 442 (sh) (360), 340 (sh) (270)	470 (690), 358 (2370), 325 (4470)	508 (10 120), 474 (9350), 435 (7680)
dmphen	510 (450), 436 (sh) (450), 378 (sh) (870), 337 (sh) (2460)	464 (500), 391 (1660), 358 (2090), 344 (3840)	485 (1880), 425 (2370)
$Hcat^-$	474 (880), 390 (sh) (1500), 350 (sh) (130), 326 (sh) (130)	618 (270), 391 (680), 365 (710), 352 (590), 342 (500)	454 (8690)
cat^{2-}	505 (280), 422 (sh) (360), 375 (sh) (620), 361 (sh) (700), 333 (1980), 324 (2390)	505 (1660), 400 (sh) (1360), 370 (1510)	464 (10 540)
$Hdbcat^-$	556 (sh) (120), 358 (820)	640 (sh) (300), 530 (510), 393 (1660)	560 (5320)
$dbcat^{2-}$	640 (100), 528 (sh) (200), 384 (860)	693 (260), 415 (sh) (1430), 383 (5530)	567 (3990)
	$[FeL^6Cl_2]\cdot H_2O$	$[FeL^7Cl_2]\cdot H_2O$	$[FeL^8Cl_3]\cdot H_2O$
None	508 (1540)	503 (1760), 410 (sh) (4350), 334 (9070)	436 (sh) (540), 358 (2780)
mim	501 (1530)	467 (1740), 410 (sh) (4040), 340 (8950)	397 (600), 340 (820)
bzim	504 (1830)	475 (1680), 410 (sh) (4290), 330 (9880)	390 (sh) (600), 350 (830)
py	515 (1510)	486 (1400), 410 (sh) (5280), 330 (11 790)	462 (180), 324 (710)
Pho^-	415 (sh) (3810), 293 (sh) (17 840)	673 (sh) (130), 614 (sh) (280), 385 (sh) (29 740), 364 (33 330)	391 (sh) (290), 283 (sh) (4120)
sal^-	380 (1030), 327 (6360)	673 (sh) (120), 377 (7220), 340 (sh) (4880)	410 (710), 370 (1800), 320 (2920), 295 (3390)
bipy	514 (17 900)	490 (2050), 337 (4040)	515 (660), 486 (620), 405 (600), 346 (1150)
phen	501 (11 380)	490 (sh) (2870), 405 (5250), 350 (sh) (8040)	505 (800), 468 (sh) (720), 444 (sh) (600)
dmphen	527 (2440)	475 (1800), 405 (2550), 350 (5210)	436 (sh) (360), 358 (sh) (890), 328 (sh) (3700)
$Hcat^-$	460 (4080)	545 (2210), 390 (4070)	614 (sh) (580), 410 (1320), 328 (1940)
cat^{2-}	508 (2490)	—	470 (850), 390 (940), 295 (4070)
$Hdbcat^-$	564 (1150)	660 (sh) (660), 390 (2510), 350 (2170)	614 (sh) (400), 495 (sh) (780), 395 (2380)
$dbcat^{2-}$	575 (1050)	650 (sh) (1710), 353 (7270)	637 (440), 456 (1210), 397 (2710)
	$[FeL^3Cl_2]\cdot H_2O$	$[FeL^4Cl_2]\cdot H_2O$[e]	
None	510 (300), 390 (sh) (1270), 365 (sh) (2020), 320 (2970)	580 (1730), 430 (sh) (1030)	

[a] Concentration of iron complexes 3.3 × 10^{-4} mol dm^{-3}. [b] The ratio of added ligands to iron complexes was 10:1 for monodentate base and 5:1 for chelating base; the anions were generated by adding 1 equivalent of methanolic NaOH to solutions containing the base and iron complex in ratio 5:1. [c] Recorded under nitrogen; the monoanions/dianions were generated by adding the corresponding amounts of methanolic NaOH to dry methanol solution. [d] Hsal = salicylaldehyde. [e] Consistent with ref. 23.

Results and Discussion

On the basis of the results of elemental analysis (Table 1) the formulae of the present iron(III) complexes may be represented as $[FeLCl_2]\cdot nH_2O$ (n = 0 or 1). In the crystal structures of $[FeL^9Cl_3]$[22] [L^9 = bis(benzimidazol-2-ylmethyl)methylamine] and $[FeL^{10}Cl_3]$[24] [L^{10} = bis(pyridin-2-ylmethyl)amine], the homologue and pyridine analogues respectively of $[FeL^8Cl_3]$, all three chloride ions are co-ordinated. So it may be expected that the chloride ions in all the present complexes are co-ordinated in the solid state and hence the iron(III) centres can achieve in solution five- or six-co-ordinate structures by binding to solvent molecules or polar groups of the neighbouring ligand molecules. Conductivity results (Λ_M, 150–200 for $[FeLCl_2]$, 310 ohm^{-1} cm^2 mol^{-1} for $[FeL^8Cl_3]$) reveal that the chloride ions are quite certainly not co-ordinated in methanol solution, at least for the monomeric species.

The present tridentate ligands provide reasonable analogues of histidine and tyrosinate co-ordination in CTD enzyme *via* the benz(imidazole) and phenolate moieties. Although the nitro group in some of the models was introduced because of the ease of synthesis of the compounds from the synthetically readily accessible benzyl chloride, it is advantageous in studying the factors affecting the charge transfer (c.t.) spectral features, adduct formation and redox behaviour. Thus in a tripodal copper(II) phenolate complex[25] the *p*-nitrophenolate moiety prefers to co-ordinate axially. Further, the present ligands are varied by saturation of the imine function to disrupt conjugation between the functionalities and to allow more flexibility in chelation to the metal ion.

In the IR spectra of the complexes with imine structures[21] ν(C=N) occurs as a medium-intensity band around 1620 cm^{-1}. The phenyl-ring vibrations, ν(C=C), are observed around

1580 cm^{-1}. A sharp ν(N–H) band around 3350 cm^{-1} is observed for compounds containing a N–H bond. The presence of lattice water is revealed by the broad shallow band around 3500 cm^{-1}.

All the iron(III) complexes have magnetic moments in the range 5.95–6.02 μ_B at room temperature, characteristic of high-spin iron(III).

Electronic Absorption Spectra.—The electronic spectra of all the iron(III) phenolate complexes in methanol solution (Table 1) exhibit two bands in the near-UV [≈410 (sh), ≈330 nm] and one in the visible (554–470 nm) region. The spectra of most of the complexes show solvent dependence; for instance, the visible band of $[FeL^5Cl_2]$ is shifted from 554 nm in methanol to 514 nm with the intensity reduced nearly to half in methanol–nitromethane (1:1 v/v). This illustrates co-ordination of methanol to iron(III) and/or different degrees of dimerisation[21] of the monomeric complexes in the solvent mixture. Hydrogen bonding between benzimidazole (bzim) NH and co-ordinated secondary amine NH on an adjacent complex may lead to the formation of a weakly bound dimeric species. The tendency towards strong hydrogen bonding of bzim[26–28] and amine[29] NH in the solid state has been noted previously. Further, the visible band observed in methanol solution exhibits significant concentration dependence; for instance, λ_{max} for $[FeL^5Cl_2]$ in methanol solution shifts from 520 to 554 nm on dilution from 3.33×10^{-4} to 1.67×10^{-4} mol dm^{-3} and there is a small change in ε_{max}.

The visible band which is absent for $[FeL^8Cl_3]$ with no phenolate co-ordination may be assigned[21] to a phenolate $(\pi_1) \longrightarrow Fe^{III}$ $[d_\pi(d_{xz})]$ c.t. transition. The complex $[FeL^8Cl_3]$ exhibits two bands which may be associated with bzim→high-spin Fe^{III} c.t. transitions but detailed studies on even imidazole (Him)→Fe^{III} ligand-to-metal charge transfer (l.m.c.t.) transitions are currently limited to low-spin complexes.[30]

The position and intensity of the visible band shows a dependency on the nature of the ligand. The increasing order of its energy, $FeL^4 < FeL^5 < FeL^1 < FeL^3 < FeL^6 < FeL^7 < FeL^2$, reflects the decreasing order of Lewis acidity of the iron(III) centre. Obviously, the metal d-orbital energies are raised[31] by the higher basicity of imine compared to –NH– nitrogen and of Him compared to bzim. Electron-donating substituents in the phenolate ring have been shown[31] to shift the visible band to higher energy. So the electron-withdrawing NO_2 group would be expected to decrease the band energy. In order to understand the observed anomalous effect of NO_2, MOPAC[32] calculations using a MNDO Hamiltonian were performed on phenolate and *p*-nitrophenolate ions the geometries of which were fully optimised. Our calculations show that for *p*-nitrophenolate ion the highest occupied molecular orbital (HOMO) π_1 and π_2 immediately below are more stable (π_1, −4.031; π_2, −6.019 eV) than those respectively of the phenolate ion (π_1, −2.527; π_2, −4.639 eV); this means that *p*-nitrophenolate is a poor electron donor. There is an n(σ) level close to π_2 in *p*-nitrophenolate (−6.154 eV) and phenolate (−4.689 eV). It is inferred from these values that both the π as well as the n(σ) level participate in c.t. transitions. It is to be noted that this is in contradiction to the earlier predictions by CNDO/2 calculations[21] on phenolate ion. Fig. 1 illustrates that the observed blue shift (compared to $[FeL^1Cl_2]$) of the visible band on introduction of a *p*-NO_2 group as in $[FeL^2Cl_2]$ is due to lowering of the energy of the ligand orbitals.

The high-intensity band observed around 400 nm for all the complexes may be assigned to charge transfer from the filled d orbitals of iron(III) (Fig. 1) to the antibonding orbitals of the phenolic residue. The more intense band near 330 nm for $[FeL^1Cl_2]$ and $[FeL^5Cl_2]$ is not observed for the respective C=N reduced complexes $[FeL^2Cl_2]$ and $[FeL^6Cl_2]$ and also for $[FeL^8Cl_3]$. So it may be due to the conjugated imine π ⟶ π* transition,[21] of the salicylaldimine residue. The intensities of all the c.t. bands in the bzim-based complexes are four-fold higher than those of their pyridine (py) analogues, probably because of improved Fe–O(phenolate) overlap,[28] effected by a change in co-ordination geometry imposed by the bzim moiety. All these observations show that the band position as well as its intensity are very sensitive to the iron environment as in the native enzyme.

Adduct Formation.—On addition of secondary donor molecules the position of the visible band of the iron(III) complexes shifts generally to higher energy with modest changes in intensity. Some significant data for all the complexes in methanol solutions are included in Table 1. Though these may be indicative of possible complications arising from incomplete adduct formation and monomer–dimer equilibria, some trends are important.

Addition of an excess (1:10) of *N*-methylimidazole (mim) shifts the visible band to higher energies with decrease in intensity for almost all the complexes. A similar change is observed upon addition of bzim but the shift in λ_{max} is comparatively less; this is expected as bzim is less basic and bulkier than mim. However, the addition of pyridine, though decreasing λ_{max}, enhances the intensity, except for the py-derived compounds $[FeL^1Cl_2]$ and $[FeL^2Cl_2]$. On adding bidentate heterocyclic bases there is a similar blue shift in λ_{max} of the visible band with a moderate to tremendous enhancement in intensity; for 2,9-dimethyl-1,10-phenanthroline (dmphen), however, there is only a slight enhancement, probably on account of steric hindrance from its methyl groups.

Addition of an excess (1:10) of phenolate and monoanionic catecholate ($Hcat^-$) ions (1:5) also brings about a large decrease in λ_{max} of the visible band with enhanced or decreased intensity for all the complexes except $[FeL^5Cl_2]$. The additional l.m.c.t. band expected for $Hcat^-$–Fe^{III} interaction may overlap with this band. Such a shift in the PhO^-→Fe^{III} c.t. bands to higher energies is clearly due to the decreased Lewis acidity of the iron(III) centre caused by the increase in number of co-ordinated phenolate donors. The latter is expected to raise the

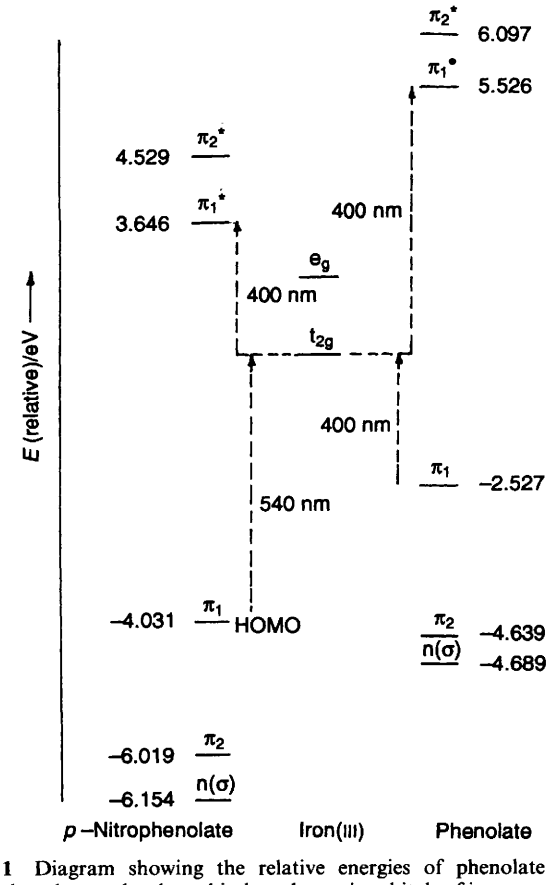

Fig. 1 Diagram showing the relative energies of phenolate and nitrophenolate molecular orbitals and atomic orbitals of iron

iron d-orbital energies, and hence the gap between the filled phenolate (π_1, π_2) and the metal t_{2g} orbitals. On the other hand, on addition of monoanionic 3,5-di-*tert*-butylcatecholate ($Hdbcat^-$), a visible band at enhanced λ_{max} with decreased intensity is observed; this suggests that monodentate $Hdbcat^-$ interacts comparatively weakly. The effect of adding dianionic cat^{2-} on the visible band is the same as that of $Hcat^-$ but the intensity is enhanced further. In contrast, the effect of addition of dianionic $dbcat^{2-}$ is to increase λ_{max} appreciably with a decrease in intensity.

Such a difference in binding of the cat and dbcat anions has not been observed for chloro(salicylidene-L-amino acidato)iron complexes;[21] this may be traced to the relative rise in energy of the π_1^* orbital (Fig. 1) by the electron-releasing *tert*-butyl substituents. The Lewis acidity of the iron centre in $dbcat^{2-}$ adducts may be arranged[16] in the following decreasing order based on the energy of the $dbcat^{2-} \rightarrow Fe^{III}$ c.t. band: $FeL^2 > FeL^7 > FeL^1 \geqslant FeL^8 > FeL^6 > FeL^5$. Though this order is not exhibited by the $cat^{2-} \rightarrow Fe^{III}$ c.t. band, the trend among the py- and bzim-containing complexes is the same. Thus the energies of the c.t. band involving the catecholates are modulated, interestingly, by the functionalities present in the primary ligand; the greater the Lewis basicity of the latter, the higher is the energy of the l.m.c.t. band involving the catechol.

EPR Spectra.—Powder samples of all the complexes exhibit broad (100–5900 G) EPR signals near $g = 4.3$ and 2.0 at room temperature (Table 2), with their relative intensities varying from complex to complex. A relatively sharp signal near $g \approx 2.0$ is exhibited in acetonitrile but not in fluid methanol solution.

The well resolved signal near $g = 4.3$ corresponds to that predicted for a transition between the middle Kramers doublet of rhombically distorted, high-spin monomeric iron(III) complexes. The linewidth of this signal varies appreciably among the present complexes. The signal found near $g = 2.0$ in fluid solutions may arise from spin–spin coupled dimeric iron(III) species.[33] The ground state of the dimer is diamagnetic and is the one solely populated at low temperature, but at high temperatures the transition in the dimeric state gives rise to this signal. Therefore in the solid state some of the iron(III) ions are weakly coupled[28] but others still give rise to EPR signals indicative of the presence of high-spin monomeric iron(III). The spectra of the complexes at room temperature and at 77 K differ only in the intensity of the high-field resonance, which decreases at low temperature due to depopulation of excited states. Thus the EPR spectra provide evidence for the existence of a monomer–dimer equilibrium. It is interesting that the $g = 2.0$ signal disappears when a donor base like pyridine or 2,2′-bipyridyl is added, but is present on addition of H_2dbcat to acetonitrile solutions of the complexes. It is evident that strong σ donors like MeCN and H_2dbcat facilitate formation of the excited state of the dimer, while solvents like methanol and π-delocalising py ligands favour the ground state.

Splitting of the $g = 4.3$ signal is observed for almost all the complexes and similar splitting is observed for transferrins,[34] a sub-class of iron(III) tyrosinate proteins, and also for simple octahedral iron(III) complexes.[35] The additional weak signal near $g = 9.05$ observed for $[FeL^5Cl_2]$ may originate from a transition involving the ground-state Kramers doublet and corresponds to that observed in diiron(III) transferrin;[36] so this complex may be a good synthetic model for transferrins also.

Table 2 Electron paramagnetic resonance spectral data for the polycrystalline iron(III) complexes at room temperature

Compound	g_2	ΔH_{pp}	g_1	ΔH_{pp}
$[FeL^1Cl_2]$	4.24	275	2.12	116
$[FeL^2Cl_2]$	—	—	2.05	175
$[FeL^3Cl_2]$	4.27	155	2.07	200
$[FeL^4Cl_2]$*	4.23	100	2.04	380
$[FeL^5Cl_2]$	4.33	493	2.07	638
$[FeL^6Cl_2]$	4.25	261	2.18	305
$[FeL^7Cl_2]$	4.25	101	2.16	392
$[FeL^8Cl_3]$	4.22	325	2.01	350

* Consistent with ref. 23.

Electrochemical Behaviour.—In methanol solution all the complexes except $[FeL^6Cl_2]$ exhibit a cathodic (0.062 to −0.630 V) as well as an anodic wave (−0.514–0.140 V, Table 3); however, for $[FeL^5Cl_2]$ no oxidation wave is discernible. The complex $[FeL^1Cl_2]$ displays an additional cathodic wave at a more positive potential (Fig. 2), probably corresponding to small amounts of iron(III) species with one co-ordinated chloride.[37] This is evident from the growth of this peak compared to the main peak, on adding an excess of tetraethylammonium chloride. For all these complexes the cathodic current functions [$D = (3.5–6.8) \times 10^{-6}$ cm^2 s^{-1}] are of the same order as those observed for a one-electron reduction process.[37] Plots of i_{pc} *vs.* $v^{\frac{1}{2}}$ ($v < 0.5$ V s^{-1}) are linear; however, the peak current ratios (i_{pa}/i_{pc}) are far from unity, suggesting irreversible charge transfer. The ΔE_p values are higher than the Nernstian value of 60 mV, implying slow electron-transfer kinetics. In contrast, $[FeL^6Cl_2]$ exhibits only one reduction wave but at a relatively more negative potential of −1.00 V with very much higher current functions; this makes us suspect the involvement of a two-electron $Fe^{III} \longrightarrow Fe^{I}$ reduction.

The Fe^{III}–Fe^{II} redox potentials of the present complexes follow the order $FeL^8 > FeL^4 > FeL^5 > FeL^1 \approx FeL^3 > FeL^7 > FeL^2$ reflecting the decrease in Lewis acidity of the iron(III) centre upon co-ordination of Lewis base phenolate and other groups with varying basicity. This trend follows that observed for the phenolate-to-iron(III) c.t. band energy and thus the complexes exhibit a linear correlation[38] between the latter and redox potential (Fig. 3).

$[FeL(dbcat)]^{n-}$. Attempted preparation of adducts of the complexes with phenolate and catecholate anions led to the isolation of materials which yielded unsatisfactory analytical results. So we generated *in situ* $[FeL(dbcat)]^{n-}$ species in which $dbcat^{2-}$ functions as a bidentate ligand as shown by spectral studies.

The cyclic voltammogram of $[FeL^1Cl_2]$ (Figs. 2 and 4) features an irreversible Fe^{III}–Fe^{II} redox process (E_{pc} −0.630 V). On adding one equivalent of H_2dbcat to $[FeL^1Cl_2]$ the irreversible dbsq ⟶ dbq oxidation wave appears near 0.508 V (Table 3) (dbsq = 3,5-di-*tert*-butyl-1,2-benzosemiquinone, dbq = 3,5-di-*tert*-butyl-1,2-benzoquinone). A new irreversible (ΔE_p 260 mV) wave with $E_{\frac{1}{2}} = -0.102$ V is observed and this corresponds to the $dbsq^-$–$dbcat^{2-}$ couple of co-ordinated[30] $dbcat^{2-}$. The irreversible reduction peak located around −0.582 V is associated with $Fe^{III} \longrightarrow Fe^{II}$ in $[FeL^1(dbcat)]$.

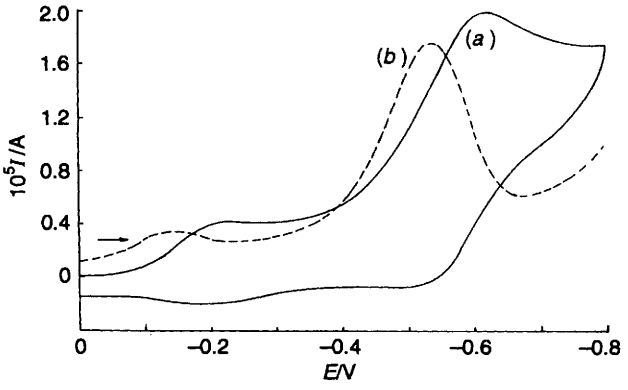

Fig. 2 Cyclic (*a*) and differential pulse (*b*) voltammograms of 1 mmol dm^{-3} $[FeL^1Cl_2]$ in methanol. Supporting electrolyte: 0.1 mol dm^{-3} $N(C_6H_{13})_4ClO_4$. Scan rates: 0.05 and 0.001 V s^{-1} respectively. Pulse height 25 mV

On adding 1, 2 (Fig. 4, Table 3) or 3 equivalents of NEt_3 the intensities of the above two reduction peaks are decreased, corresponding to deprotonation of the phenolic hydroxyl group by NEt_3 and formation of more and more [FeL^1(dbcat)]. The potential of the irreversible $dbsq^-$–$dbcat^{2-}$ couple is almost unaffected. The electrochemical data for all the [FeL(dbcat)] complexes obtained on adding 2 equivalents of NEt_3 are collected in Table 3.

The redox potential of the co-ordinated $dbsq^-$–$dbcat^{2-}$ couple[1,30] [0.049–0.615 V *vs.* normal hydrogen electrode (NHE)] is considerably more positive than that of free $dbsq^-$–$dbcat^{2-}$ couple[39] (−1.096 V *vs.* NHE) reflecting the significant stabilisation of dbcat towards oxidation upon co-ordination to Fe^{III} as well as the strong affinity[40] of catecholates for Fe^{III}, even in the absence of NEt_3 (Figs. 4 and 5). Further, these potentials are comparatively more positive than, and exhibit almost the same trend as, that of the Fe^{III}–Fe^{II} couple of the parent complexes. Thus the stabilisation of the dbcat oxidation state in

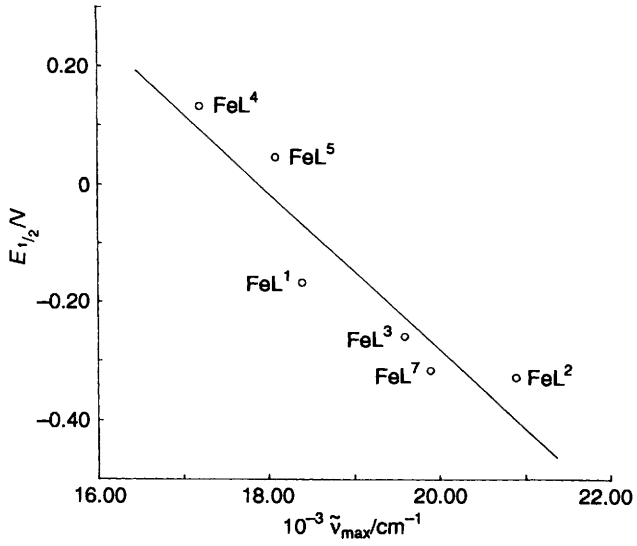

Fig. 3 Correlation of $E_{\frac{1}{2}}$ (Fe^{III}–Fe^{II}) with phenolate-to-iron(III) c.t. band energies for the iron(III) complexes

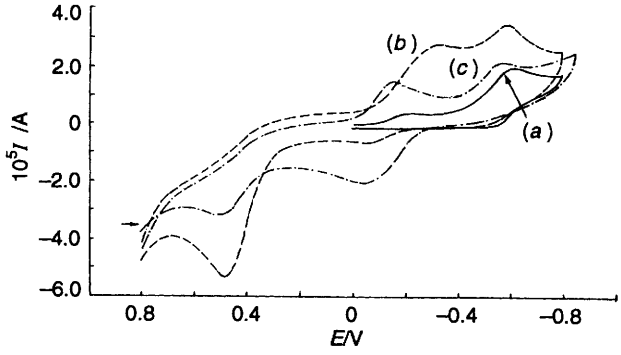

Fig. 4 Cyclic voltammograms of 1 mmol dm^{-3} [FeL^1Cl_2] (*a*), with 1 mmol dm^{-3} H_2dbcat added (*b*), and 2 mmol dm^{-3} NEt_3 added (*c*) in methanol at scan rate 0.05 V s^{-1}. Supporting electrolyte: 0.1 mol dm^{-3} $N(C_6H_{13})_4ClO_4$

Table 3 Electrochemical data[a] for the parent and $dbcat^{2-}$ bound[b] complexes in methanol at 25 ± 0.2 °C using a scan rate of 50 mV s^{-1}

Compound	E_{pc}	E_{pa}	ΔE_p/mV	$E_{\frac{1}{2}}$/V CV	$E_{\frac{1}{2}}$/V DPV[c]	i_{pc}/μA	Redox process
[FeL^1Cl_2]	−0.224				−0.169	5.2	Dimer reduction?
	−0.630	−0.514	116		−0.567	21.9	$Fe^{III} \rightarrow Fe^{II}$
[FeL^1Cl_2] + $dbcat^{2-}$		0.508			0.444		$dbsq^-$–dbq
	−0.158	−0.046	112	−0.102	−0.116	15.3	$dbsq^-$–H_2dbcat
	−0.582				−0.553	11.3	$Fe^{III} \longrightarrow Fe^{II}$
[FeL^2Cl_2]	−0.410	−0.252	158	−0.331	−0.330	13.9	$Fe^{III} \longrightarrow Fe^{II}$
[FeL^2Cl_2] + $dbcat^{2-}$		0.526			0.554		$dbsq^-$–dbq
	−0.286	−0.170	116	−0.223	−0.244	22.2	$dbsq^-$–H_2dbcat
	−0.654				−0.543	15.9	$Fe^{III} \longrightarrow Fe^{II}$
[FeL^3Cl_2]	−0.358	−0.142	216	−0.250	−0.260	12.6	$Fe^{III} \longrightarrow Fe^{II}$
[FeL^3Cl_2] + $dbcat^{2-}$		0.588			−0.640		$dbsq^-$–dbq
	−0.356	−0.200	156	−0.278	−0.277	11.8	$dbsq^-$–H_2dbcat
	−0.582				−0.519		$Fe^{III} \longrightarrow Fe^{II}$?
[FeL^4Cl_2]	−0.016	0.290	306	0.137	0.131	7.8	$Fe^{III} \longrightarrow Fe^{II}$
[FeL^4Cl_2] + $dbcat^{2-}$		0.440			0.459		$dbsq^-$–dbq
	−0.024	0.302	326		0.139	54.4	$dbsq^-$–H_2dbcat
	−0.350				−0.239		$Fe^{III} \longrightarrow Fe^{II}$
[FeL^5Cl_2]	−0.006				0.044	16.6	Dimer reduction?
	−0.231				−0.177	9.1	$Fe^{III} \longrightarrow Fe^{II}$
[FeL^5Cl_2] + $dbcat^{2-}$		0.544			0.503		$dbsq^-$–dbq
	−0.160	−0.052	108	−0.106	−0.121	11.4	$dbsq^-$–H_2dbcat
	−0.526				−0.493	6.1	$Fe^{III} \longrightarrow Fe^{II}$
[FeL^6Cl_2]	−1.000				−0.887	96.0	$Fe^{III} \longrightarrow Fe^{I}$
[FeL^6Cl_2] + $dbcat^{2-}$		0.678			0.708		$dbsq^-$–dbq
	−0.742				−0.505	36.1	$dbsq^-$–H_2dbcat
	−1.030				−0.863	30.0	$Fe^{III} \longrightarrow Fe^{II}$
[FeL^7Cl_2]	−0.276	−0.058	208		−0.319	19.2	$Fe^{III} \longrightarrow Fe^{II}$
[FeL^7Cl_2] + $dbcat^{2-}$		0.596			0.294		$dbsq^-$–dbq
	−0.300				−0.246	10.4	$dbsq^-$–H_2dbcat
	−0.646				−0.501	78.9	$Fe^{III} \longrightarrow Fe^{II}$
[FeL^8Cl_3]	0.062	0.140	78	0.101	0.101	16.7	$Fe^{III} \longrightarrow Fe^{II}$
[FeL^8Cl_3] + $dbcat^{2-}$		0.612			0.438		$dbsq^-$–dbq
	−0.002	0.126	128	0.062	0.066	27.6	$dbsq^-$–H_2dbcat
	−0.498				−0.447		$Fe^{III} \longrightarrow Fe^{II}$

[a] *E* in V *vs.* Ag–$AgNO_3$ [0.01 mol dm^{-3} $N(C_6H_{13})_4ClO_4$]; add 0.544 V to convert into values *vs.* NHE. [b] Generated by adding 1 and 2 equivalents of H_2dbcat and NEt_3 respectively to complex. [c] Pulse height 25 mV.

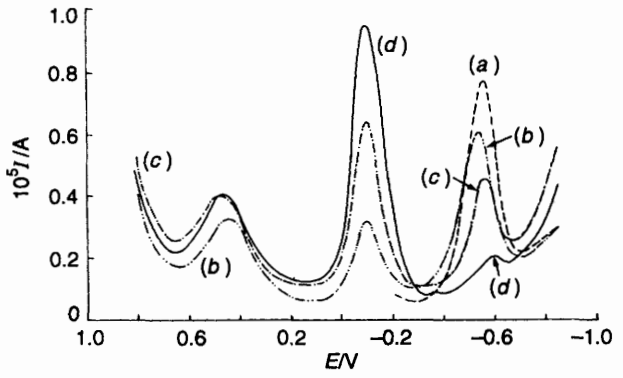

Fig. 5 Differential pulse voltammograms of 1 mmol dm^{-3} $[FeL^1Cl_2]$ (*a*), with 1 mmol dm^{-3} H_2dbcat (*b*), 1 mmol dm^{-3} NEt_3 (*c*) and 2 mmol dm^{-3} NEt_3 added (*d*), in methanol at scan rate 0.036 V s^{-1}. Supporting electrolyte: 0.1 mol dm^{-3} $N(C_6H_{13})_4ClO_4$

the substrate-co-ordinated complex is dictated by the nature of the ligand; the Lewis base NH and phenolate donors lower, while π delocalisation by NO_2 and replacement of bzim by the more π-delocalising py moiety raise, the $dbsq^-$–$dbcat^{2-}$ potential. In other words, a more Lewis acidic iron centre stabilises the dbcat oxidation state more. The trend in these potentials follows the one in the $dbcat^{2-}\rightarrow Fe^{III}$ c.t. band energies and a similar correlation has been obtained by Que *et al.*[31] These potentials are more positive (0.039–0.610 V) than that for $[Fe(salen)(dbcat)]^-$ [H_2salen = *N*,*N*′-bis(salicylidene)ethane-1,2-diamine] (−0.179 V *vs.* NHE)[41] and $[Fe(nta)(dbcat)]^{2-}$ (H_3nta = nitrilotriacetic acid) (−0.024 V, NHE);[42] while the former is unreactive towards dioxygen, the latter is the only system known thus far which exhibits catechol-cleavage activity. This suggests that all the present compounds should show cleavage activity. Further, as electron transfer from the chelated catecholate complex to dioxygen[43] is thermodynamically favoured increasingly, in decreasing order of $E_{\frac{1}{2}}$ for the $dbsq^-$–$dbcat^{2-}$ couple, $FeL^4 > FeL^1 > FeL^5 > FeL^2 \approx FeL^7 > FeL^6$, the catalytic activity and hence the yield should decrease in this order (see below).

On adding $dbcat^{2-}$, the $E_{\frac{1}{2}}$ value of the Fe^{III}–Fe^{II} couple is lowered (100–500 mV) except for $[FeL^6Cl_2]$ which exhibits an Fe^{III}–Fe^{I} process, suggesting[30] that $dbcat^{2-}$ strongly chelates to Fe^{III}. This observation is in accord with the suggestion that the iron(III) centre in the dioxygenases not only participates in the activation of the substrate but also facilitates the latter stages of the reaction. Further, the $E_{\frac{1}{2}}$ of the substrate-co-ordinated iron(III) centre reflects the reducibility of the latter to the oxide anion (Scheme 1).[43]

Catalytic Activity of Model Compounds.—The oxidative cleavage of H_2dbcat was observed in nitromethane solution when most of the model compounds were mixed with the substrate in 1:50 molar ratio and kept for 4 d. The iron(III) complexes act as catalysts in this reaction, because the yields of product (FeL^1, 19.8; FeL^2, 42.4; FeL^5, 37.0; FeL^6, 24.8; FeL^7, 23.5; FeL^8, 13.6%) were more than that of the iron(III) complex used.

The novel substrate-activation mechanism[16] (Scheme 1)* proposed by Cox and Que implies that the yield of the desired cleavage product would increase with increase in Lewis acidity of the iron centre in the substrate complex. For the present $dbcat^{2-}$ adducts the Lewis acidity as shown by the $dbcat^{2-}\rightarrow Fe^{III}$ c.t. band energies decreases in the order $FeL^2 > FeL^7 > FeL^1 \geqslant FeL^8 > FeL^6 > FeL^5$ and thus the observed yield

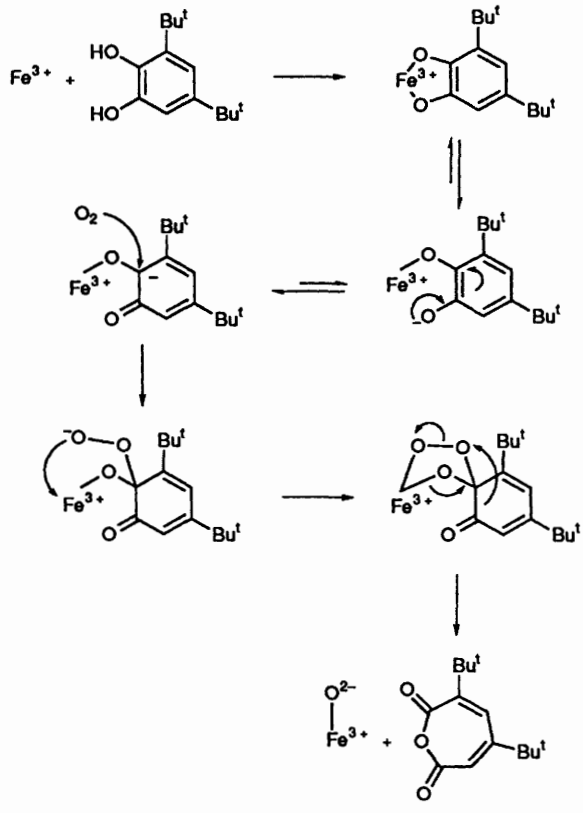

Scheme 1

also decreases in this order ($FeL^2 > FeL^7 > FeL^1 > FeL^8$) although FeL^5 and FeL^6 give higher than expected yields. The Lewis acidity as revealed by the $dbsq^-$–$dbcat^{2-}$ couple also predicts almost the same order of yield (see above), except for a few inversions and in fact a higher yield for the FeL^5 complex. Such an inconsistency in Lewis acidities predicted by spectral and electrochemical data has been observed previously.[16] Thus, as expected, the Lewis acidity of the iron(III) centre in the complex as well as in the $dbcat^{2-}$ and other adducts is modulated by the nature of the donor functionalities of the phenolate ligand. Indeed bzim, py and a NO_2 group modulate the Lewis acidity and hence the yield. As the lower yields observed for the present tridentate complexes are possibly due to the five-co-ordinate structure of the still Lewis acidic dbcat adducts, which does not encourage dissociation of one of the Fe–O (dbcat) bonds and hence the development of semiquinone character needed for the formation of the peroxide intermediate.

Relevance to Iron Oxygenases.—An important feature of the present model studies is that the phenolate-to-iron(III) c.t. band is sensitive not only to the ligand environment but also to the addends. Indeed, the visible spectra of the $dbcat^{2-}$ adducts of the complexes bear a striking similarity to those of enzyme–substrate complexes.[45–47] Since the model compounds are co-ordinatively unsaturated, the binding of H_2dbcat *or* catechol is expected to occur without replacing the already bound donors of the primary ligand. So the changes in absorption between 400 and 500 nm may be ascribed to structural changes accompanying $dbcat^{2-}$ binding and/or to the overlap of $cat^{2-}\rightarrow Fe^{III}$ c.t. bands with phenolate$\rightarrow Fe^{III}$ c.t. ones. This observation implies that in the enzyme–substrate complexes also the observed spectral change may correspond to displacement of a co-ordinated water or imidazole and not the bound tyrosinate, with no change in geometry. However, CD spectral results for the enzyme–substrate[45,47] complexes have been attributed to structural changes occurring at the iron site.

The appearance of $dbcat^{2-}\rightarrow Fe^{III}$ c.t. band and $dbsq^-$–$dbcat^{2-}$ redox wave and the depression in Fe^{III}–Fe^{II} redox

* On the basis of EPR and optical spectral studies Fujii *et al.*[44] showed that the species attacked by dioxygen is monodentate catecholate which has lost both its protons and that the charge and spin state of iron does not change during the reaction.

potential on adding H_2dbcat to the present complexes even in the absence of added base not only reveals that dbcat^{2-} is bound to the iron but also demonstrates spontaneous deprotonation of H_2dbcat on binding to iron. This is consistent with one of the suggested[31] functions of the iron(III) centre in the enzyme, *viz.* promotion of the loss of both catecholate protons. Further, this is relevant to the observation that the presence of catechol lowers the potential [as indicated[31] by the blue shift of the tyrosinate-to-iron(III) c.t. band] and renders the iron(III) centre difficult to reduce under biological conditions.[48] The observation that the yield of the desired cleavage product increases with increase in Lewis acidity of the iron centre in most of the present catecholate adducts reflects the co-ordination of the intermediate peroxide to the metal and provides support for the novel substrate-activation mechanism proposed by Cox and Que.[16] The EPR spectral features of the dbcat^{2-} adducts of the present complexes correspond to high-spin Fe^{III} rather than the semiquinone radical. Similarly, the EPR signal observed for the enzyme–substrate complexes may be due to only high-spin Fe^{III} rather than to any incipient semiquinone radical.

The present iron(III) complexes may be good models also for the iron tyrosinate protein lactoferrin, mimicking the tyrosinate-to-iron(III) c.t. spectral features and the quite negative value of $E_{\frac{1}{2}}$.

Acknowledgements

We thank the Council of Scientific and Industrial Research, New Delhi, for a fellowship (to R. V.) [9/475(25)91 EMR 1] and for supporting this research [Scheme No. 9(299)/90 EMR-II], Dr. S. Ananthapadmanabhan, Hindustan Photo Films, Ooty for C, H, N analysis and Regional Sophisticated Instrumentation Centre, Indian Institute of Technology, Madras for EPR measurements. We thank Drs. P. Venuvanalingam and R. Sumathy for MOPAC calculations.

References

1 L. Que, jun., *Adv. Inorg. Biochem.*, 1983, **5**, 167; *Struct. Bonding (Berlin)*, 1980, **40**, 39.
2 B. P. Gaber, V. Miskowski and T. G. Spiro, *J. Am. Chem. Soc.*, 1974, **96**, 6868.
3 L. Que, jun., J. D. Lipscomb, R. Zimmermann, E. Munck, W. H. Orme Johnson and N. R. Orme-Johnson, *Biochim. Biophys. Acta*, 1976, **452**, 320; J. W. Whittaker, J. D. Lipscomb, T. A. Kent and E. Munck, *J. Biol. Chem.*, 1984, **259**, 4466; T. A. Kent, E. Munck, J. W. Pyrz, J. Widom and L. Que, jun., *Inorg. Chem.*, 1987, **26**, 1402.
4 L. Que, jun., R. H. Heistand, II, R. Mayer and A. L. Roe, *Biochemistry*, 1980, **19**, 2588; L. Que, jun. and R. M. Epstein, *Biochemistry*, 1981, **20**, 2545.
5 R. H. Felton, W. L. Barrow, S. W. May, A. L. Sowell and S. Goel, *J. Am. Chem. Soc.*, 1982, **104**, 6132.
6 J. W. Whittaker and J. D. Lipscomb, *J. Biol. Chem.*, 1984, **259**, 4487.
7 R. H. Felton, L. D. Cheung, R. S. Phillips and S. W. May, *Biochem. Biophys. Res. Commun.*, 1978, **85**, 844; W. E. Keyes, T. M. Loehr, M. L. Taylor and J. S. Loehr, *Biochem. Biophys. Res. Commun.*, 1979, **89**, 420.
8 L. Que, jun. and R. H. Heistand, II, *J. Am. Chem. Soc.*, 1979, **101**, 2219.
9 T. A. Walsh, D. P. Ballou, R. Mayer and L. Que, jun., *J. Biol. Chem.*, 1983, **258**, 14422.
10 T. Funabiki, H. Sakamoto, S. Yoshida and K. Tamara, *J. Chem. Soc., Chem. Commun.*, 1979, 754.
11 M. Matsumoto and K. Kuroda, *J. Am. Chem. Soc.*, 1982, **104**, 1433.
12 Y. Tatsuno, M. Tatsuda and S. Otsuka, *J. Chem. Soc., Chem. Commun.*, 1982, 1100.
13 M. G. Weller and U. Weser, *J. Am. Chem. Soc.*, 1982, **104**, 3752; 1985, **107**, 243.
14 Y. Nishida, H. Shimo and S. Kida, *J. Chem. Soc., Chem. Commun.*, 1984, 611.
15 L. Que, jun., *Coord. Chem. Rev.*, 1983, **50**, 73.
16 D. Cox and L. Que, jun., *J. Am. Chem. Soc.*, 1988, **110**, 8085.
17 J. C. Davis, W.-J. Kung and B. A. Averill, *Inorg. Chem.*, 1986, **25**, 394; L. Que, jun., R. H. Heistand, II, R. Mayer and A. L. Roe, *Biochemistry*, 1980, **19**, 2588.
18 T. M. Aminabhavi, N. S. Biradar and S. B. Patil, *Inorg. Chim. Acta*, 1986, **125**, 125.
19 *Organic Synthesis*, ed. E. C. Horning, Wiley, New York, 1955, vol. 3, p. 468.
20 S. Usha, T. Pandiyan and M. Palaniandavar, *Indian J. Chem.*, 1992, **55**, 878.
21 L. Casella, M. Gullotti, A. Pintar, L. Messouri, A. Rockenbauer and M. Gyor, *Inorg. Chem.*, 1987, **26**, 1031.
22 H. Adams, N. A. Bailey, J. D. Crane, D. E. Fenton, J. M. Latour and J. M. Williams, *J. Chem. Soc., Dalton Trans.*, 1990, 1727.
23 T. R. Demmin and M. M. Rogic, *J. Org. Chem.*, 1980, **45**, 4072.
24 R. Viswanathan, M. Palaniandavar, T. Balasubramanian and P. Thomas Muthiah, unpublished work.
25 R. Uma, R. Viswanathan, M. Palaniandavar and M. Lakshminarayanan, *J. Chem. Soc., Dalton Trans.*, 1994, 1219.
26 S. B. Sanni, H. J. Behm, P. T. Beurskens, G. A. Van Albada, J. Reedijk, A. T. H. Lenstra, A. W. Addison and M. Palaniandavar, *J. Chem. Soc., Dalton Trans.*, 1988, 1429.
27 A. W. Addison, P. J. Burke, K. Henrick, T. N. Rao and E. Sinn, *Inorg. Chem.*, 1983, **22**, 3645.
28 M. R. McDevitt, A. W. Addison, E. Sinn and L. K. Thompson, *Inorg. Chem.*, 1990, **29**, 3425.
29 M. Palaniandavar, T. Pandiyan, M. Lakshminarayanan and H. Manohar, *J. Chem. Soc., Dalton Trans.*, 1995, 455.
30 C. R. Johnson, W. W. Henderson and R. F. Shepherd, *Inorg. Chem.*, 1984, **23**, 2754.
31 L. Que, jun., R. C. Kolanczyk and L. S. White, *J. Am. Chem. Soc.*, 1987, **109**, 5373.
32 J. J. P. Stewart, *J. Comput. Chem.*, 1989, **10**, 209.
33 L. Borer, L. Thalken, C. Ceccarelli, M. Glick, J. Zhang, II and W. M. Reiff, *Inorg. Chem.*, 1983, **22**, 1719; L. Borer, L. Thalken, J. Zhang, II and W. M. Reiff, *Inorg. Chem.*, 1983, **22**, 3174.
34 I. W. Ainscough, A. M. Brodie, J. F. Plowman, S. J. Bloor and S. J. Loehr, *Biochemistry*, 1980, **19**, 4072.
35 W. T. Oosterhuis, *Struct. Bonding (Berlin)*, 1974, **20**, 59; M. I. Scullane, L. K. White and N. O. Chasteen, *J. Magn. Reson.*, 1982, **47**, 383; R. Aasa, *J. Chem. Phys.*, 1970, **52**, 3919; M. D. Stallings and D. T. Sawyer, *J. Am. Chem. Soc.*, 1980, **102**, 4481.
36 R. Aasa, B. G. Malmstroms, P. Saltman and T. Vanngard, *Biochim. Biophys. Acta*, 1963, **75**, 203.
37 T. Pandiyan, M. Palaniandavar, M. Lakshminarayanan and H. Manohar, *J. Chem. Soc., Dalton Trans.*, 1992, 3377.
38 K. Ramesh and R. N. Mukherjee, *J. Chem. Soc., Dalton Trans.*, 1992, 83.
39 E. J. Nanni, M. D. Stallings and D. T. Sawyer, *J. Am. Chem. Soc.*, 1980, **102**, 4481.
40 A. Avdeef, S. R. Sofen, T. C. Bregante and K. N. Raymond, *J. Am. Chem. Soc.*, 1978, **100**, 5362.
41 R. B. Lauffer, R. H. Heistand, II and L. Que, jun., *J. Am. Chem. Soc.*, 1981, **103**, 3947.
42 L. S. White, L. H. Nilsson, L. H. Pignolet and L. Que, jun., *J. Am. Chem. Soc.*, 1984, **106**, 8312.
43 L. Que, jun., J. D. Lipscomb, E. Munck and J. M. Wood, *Biochim. Biophys. Acta*, 1977, **485**, 60.
44 S. Fujii, H. Ohya-Nishiguchi, N. Hirota and A. Nishinaga, *Bull. Chem. Soc. Jpn.*, 1993, **66**, 1408.
45 M. Nozaki, *Top. Curr. Chem.*, 1979, **78**, 145.
46 L. Que, jun., *J. Chem. Educ.*, 1985, **62**, 938.
47 B. Nagy, J. P. Aubert, M. II. Loucheux-Lefevre and G. Spik, *FEBS Lett.*, 1976, **66**, 238.
48 J. W. Pyrz, A. L. Roe, L. J. Stern and L. Que, jun., *J. Am. Chem. Soc.*, 1985, **107**, 614.

Received 18*th August* 1994; *Paper* 4/05063K